# CHARACTERISTICS OF THE SEA SURFACE DISTURBANCE INDUCED BY THE RAYLEIGH WAVES*

**Shusaku Inoue** and **Tatsuo Ohmachi**

Tokyo Institute of Technology, Department of Built Environment, Japan
E-mail: **shusaku@enveng.titech.ac.jp**

## 1. INTRODUCTION

In recent years, serious damage has been caused by near-field tsunamis whose arrival time is less than or equal to a few minutes after the occurrence of the earthquake. Current tsunami warning systems need at least several minutes to announce tsunami warning because these systems are normally based on detection of submarine faults from the seismic data observed at several points. The wave heights estimated from the real time tsunami warning system frequently do not correspond to the actual wave heights at a near-field area because of approximations used in their estimation.

To develop a new tsunami warning system that is faster and more accurate than the current system we aimed to use the sea surface disturbance induced by the Rayleigh wave, which precedes tsunami waves. The purpose of this study is to examine the possibility of the tsunami warning based on observations of the Rayleigh wave and associated sea surface disturbances. For this purpose, we investigated the characteristics of the Rayleigh wave and the sea surface disturbance both by numerical simulation and by using the real observational data.

The tidal record shown in Figure 1 is the wave observed at Fukaura during the 1983 Nihonkai-Chubu Earthquake. Because the main purpose of tide gauges is to record tides, the chart speed is very slow. This interval is 1 hour. From the record in Figure 1 we can see that long period waves arrived after 12 o'clock. These recorded waves were related to the tsunamis, which attacked Fukaura. We can also see another wave "high-frequency" with an amplitude of 44 cm arrived 7 minutes before the tsunami. This wave is associated with the sea surface disturbance preceding tsunami.

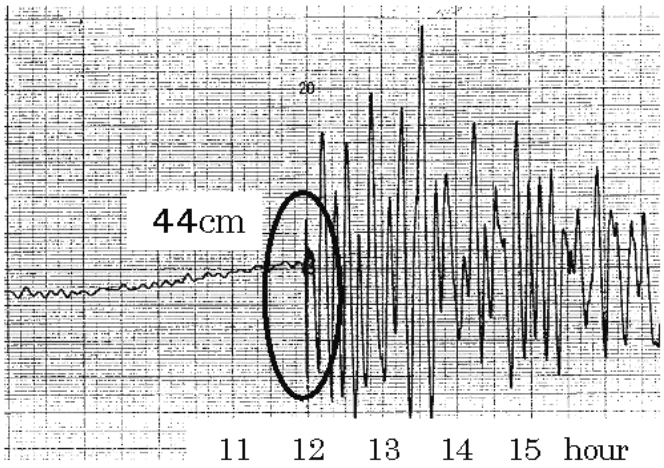


Figure 1. Tidal record at Fukaura after the 1983 Nihonkai-Chubu Earthquake

## 2. TWO-DIMENSIONAL TSUNAMI SIMULATION

Our simulation technique is different from the conventional technique based on the static seabed displacement and long wave approximation. First, we simulate dynamic displacements of seabed

* Edited by A. B. Rabinovich and W. Rapatz.

by the Boundary Element Method (BEM). Then we input the vertical velocity of the displacement to the seabed of the fluid domain. Propagation of the sea-surface disturbance is simulated by the finite difference method. In this simulation, we use the Navier-Stokes equations, which enable us to account for acoustic effects [Ohmachi *et al*., 2001].

To investigate the characteristics of the sea surface disturbance, we simulated two-dimensional propagation of a tsunami. Figure 2 illustrates the analytical model employed. We assumed that the tsunami source was a thrust fault 30 km in width, dipping at 30 degrees, and located 7 km under the seabed. This fault undergoes unilateral faulting, which means that the fault rupture starts at the bottom and propagates upward. The rupture velocity, dislocation, and rise time are shown in Figure 2. The water depth above the seabed is 3 km, and the area considered in the calculation extends to ±100 km from the fault.

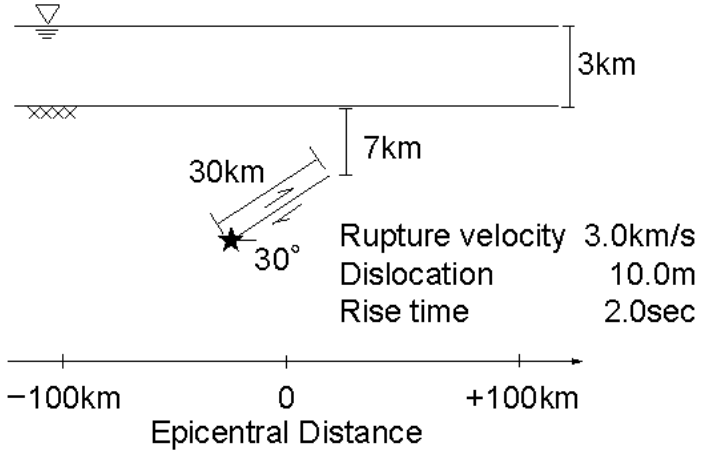


Figure 2. 2-D tsunami simulation model.

Snapshots in a few seconds after the fault rupturing are shown in Figure 3. The lower and upper surfaces represent the seabed and the sea surface, respectively. The wave height in the near-fault area 15 sec after the fault rupturing became bigger than the seabed displacement. From 20 to 30 sec, the Rayleigh waves are generated in the near-fault area, propagating along the seabed, to the right of the figure. Short period forced sea surface waves propagate with the same speed as these Rayleigh waves, which is significantly higher than the long-wave speed of tsunami propagation. From this simulation, we can point out that the sea surface disturbances preceding tsunami waves are generated by the Rayleigh waves.

## 3. CHARACTERISTICS OF PROPAGATION

### *3.1. The 1993 Hokkaido-Nansei-Oki tsunami*

In our new tsunami warning system, we propose to develop a single point observation system. So, it is very important to know how the Rayleigh wave propagates from the source area. To investigate the characteristic of the propagation, we check the tidal records of the 1993 Hokkaido-Nansei-Oki tsunami, and the seismic data of the 1999 Chi-Chi Taiwan earthquake.

Figure 4 shows wave height distribution of the sea surface disturbances observed after the 1993 Hokkaido-Nansei-Oki Earthquake. In this figure, black circles show tidal observation sites and wave heights are indicated in cm. The fault model proposed by Mendoza and Fukuyama [1996] has northern and southern faults. In this model, the fault rupturing starts at the northern fault and propagates to the southern fault. Black stars are the epicenters of the faults. From this figure it follows that the sea surface disturbances are observed in the limited area from Iwanai to Noshiro. The observed sea surface disturbances trend to the south. We thought that this occurs because the Rayleigh wave increases gradually as the fault rupturing propagates from the Northern Fault to the Southern Fault. The Rayleigh wave propagates through the ground, so the sea surface disturbances associated with this wave are observed in Mori where tsunami have not arrived.

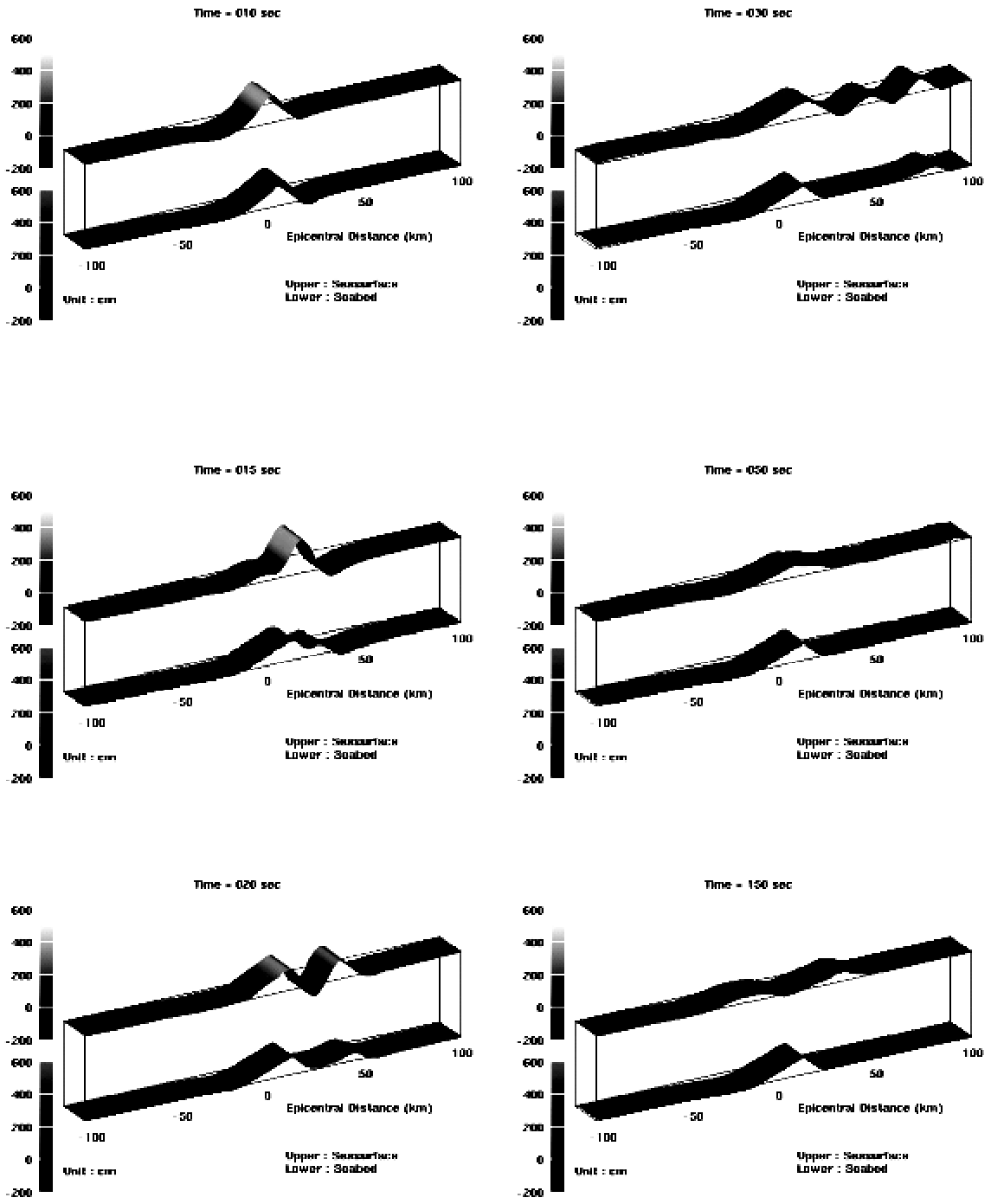


Figure 3. Two-dimensional tsunami simulation.

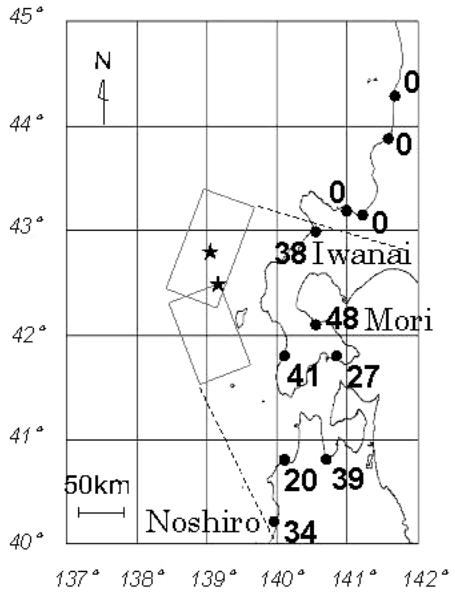


Figure 4. Wave height distribution of sea surface disturbance.

### *3.2. The 1999 Chi-Chi Taiwan Earthquake*

The 1999 Chi-Chi Taiwan Earthquake is a low-angle thrust-faulting earthquake with $M_s$ = 7.6 (USGS) occurred in central Taiwan on September 20, 1999. Thrust-faulting subduction earthquakes frequently cause tsunamis, but the seismic data of this type have not been recorded before. For this reason, despite knowing that this earthquake had not generated tsunami waves, we use this earthquake in the present study.

Digital seismic acceleration data, that include 441 points around Taiwan, were provided by Lee *et al*. [2001]. Figure 5 shows these observation stations and the fault projection for the model proposed by Kikuchi *at el*. [2000]. This fault model is a low-angle thrust faulting; the slope is inclined eastward. To find the displacement by the Rayleigh wave, we simply integrated the vertical acceleration records after filtering with the bandpass filter from 2 to 20 sec.

The distribution of maximum displacements is shown in Figure 6. According to this figure, the displacement is bigger on the northwestern side of the fault than on the other side. The area of large displacement is limited to the frontal zone of the fault. The epicenter of this earthquake is located in the center of this fault. We assume that the Rayleigh wave increases gradually on the west side where the fault rupturing propagates into the shallower area and does not increase on the east

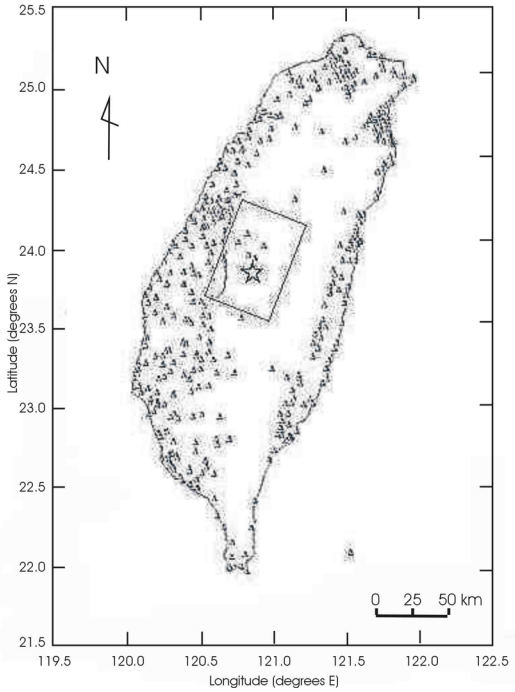


Figure 5. Observation sites and projection of the fault plane.

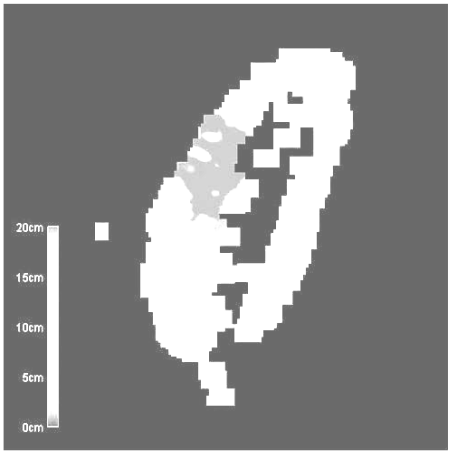


Figure 6. Distribution of maximum displacement.

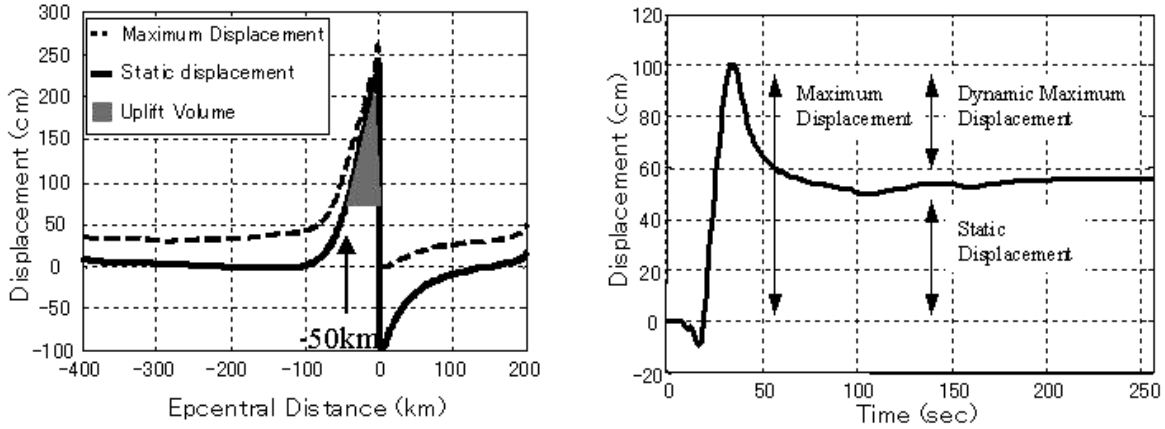


Figure 7. Uplift volume of the ground and the dynamic maximum displacement.

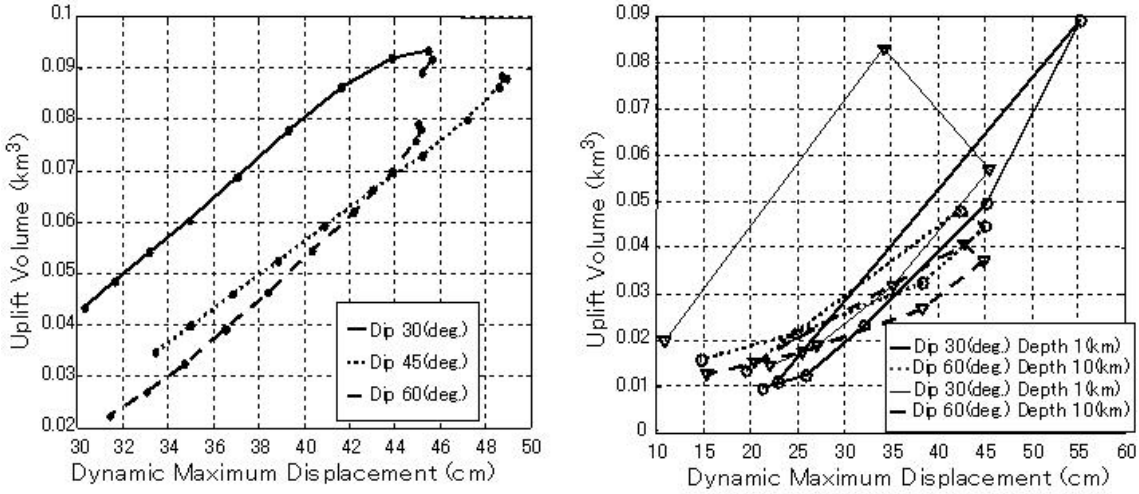


Figure 8. A correlation between uplift volume and dynamic maximum displacement.

(deeper) side. This result shows that the amplitude of the Rayleigh wave increases in the direction of the fault rupturing and in the front of the fault.

## 4. CORRELATION BETWEEN THE GROUND MOTION AMPLITUDE AND THE SEA-BED UPLIFT VOLUME

We assume that the sea surface disturbance preceding tsunami waves is generated by the Rayleigh wave. To examine the possibility of tsunami warning based on using the Rayleigh wave we estimated the correlation between the ground displacement and the volume of the seabed uplift (Figure 7). The uplift volume is estimated at an observational point 50 km away and shown as a shaded area in the left figure. The dynamic displacement of the ground is reconstructed from the static displacement (Figure 7).

Figure 8 shows the relationship between the dynamic displacement and the volume for dip angles 30, 45, and 60 degrees and changing fault depths. From the left figure we see the high correlation of these parameters. The right plot in Figure 8 shows a similar relationship for the changing fault widths. In this case the correlation is also significant. This high correlation was found on the

hanging wall side in the near-field area. However, the correlation becomes low in the far-field area or on the foot wall side.

## CONCLUSIONS

As conclusions, we would like to remark the following:

1. The Rayleigh wave generates the sea surface disturbance which propagates faster than tsunami waves.
2. The amplitude of the Rayleigh wave increases in the direction of the fault rupturing and in the front area of the fault.
3. The correlation between the dynamic maximum displacement and the uplift volume was found to be high in the near-field area of the hanging wall side but low in the far-field area.

## REFERENCES

Ohmachi T., H. Tsukiyama and H. Matsumoto (2001) : Simulation of tsunami induced by dynamic displacement of seabed due to seismic faulting, *Bull. Seism. Soc. Am.*, 91, 6, pp. 1898-1909.

Mendoza, C. and E. Fukuyama(1994) : The July 1993 Hokkaido-Nansei-Oki, Japan, earthquake : Coseismic slip pattern from strong-motion and teleseismic recordings, *J. Geophys. Res*., Vol. 101, pp. 791-801

Lee, W. H. K., T. C. Shin, K. W. Kuo, K. C. Chen and C. F. Wu(2001) : CWB free-field strong-motion data from the 921 Chi-Chi earthquake: processed acceleration files on CD-ROM, Central Weather Bureu, Taiwan.

Kikuchi, M., Y. Yagi and Y. Yamanaka(2000) : Source process of the Chi-Chi, Taiwan earthquake of September 21, 1999 inferred from teleseismic body waves, *Bull. Earthq. Res. Inst.* Vol. 75, pp. 1-13.